Trop J Nat Prod Res, December 2025; 9(12): 5955 - 5963

ISSN 2616-0684 (Print)
ISSN 2616-0692 (Electronic)

Tropical Journal of Natural Product Research

Available online at https://www.tjnpr.org

Original Research Article

Computational Insights into *Ludwigia* L. Phytochemicals as Potential PDE4B Inhibitors: Molecular Docking and Dynamics Simulations

Hoang V. Hung[1], Nguyen Hoang[2], Vu H. Son[2], Vu T. T. Le[2]*, Ngu T. T. Giang[3], Cao H. Le[2]*

[1]*Center for Interdisciplinary Science and Education, Thai Nguyen University, Thai Nguyen City, Vietnam*
[2]*Thai Nguyen University of Agriculture and Forestry, Quyet Thang, Thai Nguyen, Vietnam*
[3]*Department of Chemistry, Vinh University, Vinh City, Nghe An, Vietnam*

ARTICLE INFO

Article history:
Received 15 July 2025
Revised 28 August 2025
Accepted 30 August 2025
Published online 01 January 2026

ABSTRACT

Phosphodiesterase 4B (PDE4B) is an enzyme that regulates inflammatory responses and has recently gained attention as a promising therapeutic target for the treatment of inflammatory diseases. However, the discovery of selective and safe PDE4B inhibitors remains a challenge. The present study aimed to investigate phytochemicals derived from *Ludwigia* L. as potential PDE4B inhibitors using a combination of computational approaches. A set of compounds was initially screened based on Lipinski's Rule to assess drug-like properties, with particular emphasis on oral bioavailability and absorption. Toxicity evaluation using LD_{50} values was performed to categorize the compounds according to safety levels. Molecular docking analysis revealed that several phytochemicals exhibited strong binding affinities toward PDE4B, notably quercetin-3-O-α-L-rhamnoside, luteolin-8-C-glycoside, betulonic acid, (23E)-feruloylhederagenin, and (23Z)-feruloylhederagenin, with compound (23E)-feruloylhederagenin demonstrating the highest docking score (10.88 kcal/mol). Molecular dynamics simulations further confirmed the structural stability of the ligand–protein complexes, with root mean square deviation (RMSD) values consistently below 0.2 nm. Additionally, MMGBSA binding energy calculations supported the strong interaction profile of compound (23E)-feruloylhederagenin, yielding a binding free energy of -54.22 kcal/mol. Taken together, these findings provide computational evidence that *Ludwigia* L. phytochemicals, particularly (23E)-feruloylhederagenin, represent promising leads for PDE4B inhibition and may serve as valuable candidates for the development of novel anti-inflammatory agents.

Keywords: *Ludwigia* L., Phosphodiesterase 4B, molecular docking, molecular dynamics.

Introduction

The genus *Ludwigia* L., belonging to the *Onagraceae* Juss. family, comprises 87 accepted species, including *Ludwigia affinis*, *Ludwigia africana*, *Ludwigia alata*, *Ludwigia arcuata*, among others [1]. Several species have been recorded as traditional medicinal plants used to treat various ailments. For instance, *L. adscendens* is employed for treating ulcers and skin diseases, as well as exhibiting anti-dysenteric, anthelmintic, diuretic, antiseptic, and anti-inflammatory properties [2, 3, 4]. *L. octovalvis* has been used in the treatment of diabetes, edema, nephritis, dermatological conditions, and hypertension [5,6,7,8]. Meanwhile, *L. hyssopifolia* is known for its effectiveness against diarrhea, dysentery, bloating, leucorrhea, hemoptysis, and also acts as a deworming agent and laxative [9]. Studies have shown that *Ludwigia* species contain diverse bioactive compounds, including flavonoids, triterpenes, phenolic compounds, and saponins, which contribute to their pharmacological properties. Among the many molecular targets associated with inflammation and immune response, phosphodiesterase 4 (PDE4) stands out as a crucial enzyme family that regulates cyclic nucleotide signaling by hydrolyzing adenosine or guanosine 3',5'-cyclic phosphate (cAMP or cGMP) into their inactive forms, 5'-AMP and 5'-GMP [10,11].

*Corresponding author. Email: vuthithule@tuaf.edu.vn
Tel: +8479220483

Citation: Hoang HV, Nguyen H, Vu HS, Le VTT, Ngu TTG, Le CH. Computational Insights into *Ludwigia* L. Phytochemicals as Potential PDE4B Inhibitors: Molecular Docking and Dynamics Simulations. Trop J Nat Prod Res. 2025; 9(12): 5955 – 5963 https://doi.org/10.26538/tjnpr/v9i12.7

Official Journal of Natural Product Research Group, Faculty of Pharmacy, University of Benin, Benin City, Nigeria

PDE4 is predominantly expressed in immune and inflammatory cells, playing a pivotal role in modulating inflammatory responses. Consequently, PDE4 inhibitors have shown great promise in the treatment of various inflammatory and autoimmune diseases, such as asthma, chronic obstructive pulmonary disease (COPD), rheumatoid arthritis, psoriasis, and inflammatory bowel diseases. The PDE4 enzyme family consists of four subtypes: PDE4A, PDE4B, PDE4C, and PDE4D, each of which is highly expressed in immune cells, the central nervous system (CNS), and smooth muscle tissues, particularly in the lungs [12, 13, 14]. Among them, phosphodiesterase 4B (PDE4B) plays a critical role in immune cell signaling and inflammatory processes [15]. Selective inhibition of PDE4B has garnered significant attention due to its potential to offer therapeutic benefits while minimizing side effects commonly associated with non-selective PDE4 inhibition [16]. However, designing highly selective PDE4B inhibitors remains a considerable challenge due to the structural similarity among PDE4 subtypes [17, 18]. To address this issue, structural and computational studies including receptor- and ligand-based approaches have been utilized to enhance the binding affinity and selectivity of PDE4B inhibitors. Given the traditional medicinal applications of *Ludwigia* species and their rich phytochemical diversity, there is considerable interest in exploring their potential as natural sources of PDE4B inhibitors. Computational techniques such as molecular docking and molecular dynamics (MD) simulations are particularly relevant in this context, as they provide mechanistic insights into ligand–receptor interactions, stability, and inhibitory potential, thus accelerating drug discovery**.** To the best of our knowledge, this is the first comprehensive study integrating phytochemicals of *Ludwigia* with computational strategies to assess their potential as selective PDE4B inhibitors. This research not only bridges traditional medicinal knowledge and modern drug discovery but also highlights promising bioactive candidates from *Ludwigia* that could serve as lead compounds for the development of novel anti-inflammatory therapeutics.

ISSN 2616-0684 (Print)
ISSN 2616-0692 (Electronic)

Materials and Methods

Drug-likeness and toxicity

The physicochemical properties of natural compounds derived from *Ludwigia* species were preliminarily screened based on key criteria outlined in Lipinski's Rule of Five using the online platform Supercomputing Facility for Bioinformatics & Computational Biology (https://www.scfbio-iitd.res.in/software/drugdesign/lipinski.jsp) [19, 20]. This assessment helped evaluate the drug-likeness and oral bioavailability of the compounds. Furthermore, toxicity parameters, including LD_{50} values and oral toxicity levels, were predicted using the ProTox 3.0 online tool (https://tox.charite.de/protox3/?site=compound_input) [21]. These predictions provided insights into the potential safety and toxicity profiles of the studied compounds, contributing to the selection of promising candidates for further investigation.

Molecular docking

The structures of natural compounds derived from *Ludwigia* L. species were gathered from previous research articles and sketched using Marvin Sketch software[37, 38, 39.These] structures, along with the co-crystallized ligand, underwent energy minimization using the MMFF94s force field, computed automatically via the "obminimize" command in the OpenBabel package [22, 23]. Furthermore, their geometries were further optimized using density functional theory (DFT) at the B3LYP/6-311++G (d, p) level of theory with the ORCA software package. To prepare the structural coordinates of the human phosphodiesterase 4B (PDE4B) protein, data were retrieved from the RCSB Protein Data Bank (PDB ID: 4KP6) [24]. The protein structure was then refined by adding polar hydrogens and assigning Kollman charges using AutoDockTools v1.5.6 software. The docking protocol was established by defining the search space and setting specific grid box parameters, with coordinates at x = -41.8 Å, y = 91.2 Å, z = 114.4 Å, a grid box size of 24 × 24 × 24, and a grid spacing of 1 Å. The AutoDock Vina v1.2.3 program was used for molecular docking simulation with default parameters and an exhaustiveness of 400 [25, 26]. To ensure the reliability of the docking protocol, a validation step was performed by re-docking the original co-crystallized ligand to assess its ability to reproduce the native binding pose. After successful validation, the protocol was employed to screen the target protein PDE4B against the selected compounds. The docking results were analyzed based on binding affinity, and the top-ranked poses were selected for further investigation. Additionally, the compounds were ranked according to their binding affinity values (kcal/mol) and compared with a reference compound. The best binding poses of the highest-ranked compounds were further analyzed and visualized using Discovery Studio Visualizer software.

Molecular dynamics

Molecular dynamics (MD) simulations were conducted for the enzyme-ligand complexes (PDE4B-2, PDE4B-6, PDE4B-49, PDE4B-45, and PDE4B-51) using the GROMACS software package [27]. The AMBER99SB-ILDN force field was employed to generate the protein topology, while the Generalized AMBER Force Field 2 (GAFF2) was applied to parameterize the ligands, characterized using the Antechamber program. Each simulation began with an initial complex configuration derived from the docking poses obtained in the molecular docking protocol. The complexes were then solvated in a triclinic box using the TIP3P water model (1 nm) under periodic boundary conditions and neutralized with counterions. Before running the simulations, energy minimization was performed using the steepest descent algorithm for 50,000 steps to remove steric clashes and optimize the system. Following minimization, the systems were equilibrated through a two-step process: first, 100 ps of NVT equilibration at 300K, followed by 100 ps of NPT equilibration at 1 bar to stabilize pressure and temperature. The production MD simulations were then carried out for 100 ns to track structural changes and evaluate the stability of enzyme-ligand interactions over time. Structural analyses were performed using Excel software, while binding free energy calculations for each complex were carried out using the MMGBSA approach with the gmx_MMPBSA program [28].

Results and Discussion

Drug-likeness and toxicity assessments

The Lipinski Rule is widely applied in compound screening to assess absorption potential and oral bioavailability. This rule provides key criteria for predicting whether a compound possesses drug-like properties. If a compound violates multiple criteria, it is likely to have poor absorption, leading to a higher failure rate in clinical trials. By applying this rule, researchers can eliminate unsuitable compounds early in the drug discovery process, optimizing molecular design while saving both time and research costs. A compound is considered to have good absorption if it meets at least two of the five Lipinski criteria: a molecular weight below 500 Da, no more than five hydrogen bond donors, no more than ten hydrogen bond acceptors, a LogP value under 5, and a molar refractivity between 40 and 130 [29]. Based on the data in Table 1, several compounds, including 1, 8, 12, 21-35, 64, 65, 69, and 70, fully comply with Lipinski's Rule. These compounds are predicted to have good oral bioavailability, making them strong candidates for drug development. Additionally, compounds such as 2-5, 7, 10, 13-19, 36, 38-46, 52, 53, 63, and 66-68 satisfy at least two of the rule's criteria. Although they may not strictly follow all requirements, they remain viable for oral drug development, as further experimental studies could identify potential transport mechanisms or structural modifications to improve their absorption. In contrast, the remaining compounds are not considered for further computational simulations, as they either have excessively high molecular weights or LogP values beyond the acceptable range. These properties can negatively impact solubility and membrane permeability, hindering absorption. Notably, compounds with extremely high LogP values tend to be strongly hydrophobic, which can interfere with solubility and transport within the body. Similarly, those with molecular weights significantly exceeding 500 Da may struggle to cross cell membranes due to their large size and limited diffusion capacity. Beyond absorption, the toxicity of compounds derived from *Ludwigia* L. species was also evaluated through LD_{50} values to assess potential risks. The data indicate that highly toxic compounds include 1, 15, 17, 19, 59, 66, 67, and 68, with LD_{50} values ranging from 51 to 159 mg/kg (Table 1). Classified as Class 3, these compounds pose significant safety concerns and require careful consideration in further research. Moderately toxic compounds, including 8, 16, 18, 20, 21, 22, 24, 25, 28, 30, 31, 33, 36, 38, 41, 45, 47, 48, 60, 61, 62, and 65, have LD_{50} values between 750 and 2000 mg/kg and fall into Class 4. While these compounds exhibit moderate toxicity, they can still be explored for drug development, provided that dosage and handling precautions are taken into account. In contrast, the majority of the remaining compounds, such as 2-7, 9-14, 23, 26, 27, 29, 32, 34, 35, 37, 39, 40, 42, 43, 44, 46, 49-58, 63, 64, 69, and 70, demonstrate low toxicity with LD_{50} values exceeding 2000 mg/kg. Falling into Class 5-6, these compounds present minimal safety concerns, making them promising for further investigation. Through a combination of Lipinski's Rule-based screening and toxicity prediction, compounds that meet at least two criteria while maintaining moderate toxicity levels (Class 4 or higher) were selected for further studies. These compounds will undergo molecular docking and dynamics simulations to evaluate their potential as PDE4B enzyme inhibitors, paving the way for future drug development efforts.

Molecular docking results

To identify compounds derived from *Ludwigia* L. species that exhibit potential PDE4B inhibitory activity, a molecular docking approach was employed to screen and evaluate binding affinity and interaction modes for subsequent biological experimental studies. Before conducting the screening, the effectiveness of the docking protocol was assessed by redocking the co-crystallized ligand of PDE4B (PDB ID: 4KP6) into its binding site to determine the reliability of the predicted pose. As shown in Figure S2, the redocked ligand exhibited good overlap between the docked conformations and the original co-crystallized ligand structure, with an RMSD value of 1.82392 Å, which is below the 2 Å threshold, indicating high reliability of the current docking protocol [30]. Next, this docking protocol was used to dock the studied compounds against the PDE4B protein to evaluate their inhibitory potential.

ISSN 2616-0684 (Print)
ISSN 2616-0692 (Electronic)

Table 1: Drug-likeness based on Lipinski's rule of five and toxicity of studied compounds

Compounds	MW	HBD	HBA	LOGP	MR	Number of violations	LD_{50}	Toxicity class
1	302	5	7	2.010899	74.050476	0	159	3
2	448	7	11	0.296999	104.862053	2	5000	5
3	434	7	11	-0.091501	100.267052	2	5000	5
4	464	8	12	-0.730601	106.273849	2	5000	5
5	434	7	11	-0.091501	100.267052	2	5000	5
6	608	9	15	-0.603601	140.652725	4	5000	5
7	464	8	12	-0.730601	106.273849	2	5000	5
8	304	5	7	1.186299	73.249474	0	2000	4
9	684	8	16	2.6685	162.990555	4	5000	5
10	464	8	12	0.0026	106.526848	2	5000	5
11	698	9	16	2.628	168.535385	4	5000	5
12	286	4	6	2.305299	72.385674	0	3919	5
13	448	7	11	-0.436201	104.609047	2	5000	5
14	448	7	11	-0.436201	104.609047	2	5000	5
15	318	6	8	1.7165	75.715271	1	159	3
16	448	8	11	-0.359901	105.198853	2	1213	4
17	448	8	11	-0.359901	105.198853	2	159	3
18	432	7	10	-0.065501	103.53405	1	832	4
19	432	7	10	-0.065501	103.53405	1	159	3
20	558	7	11	4.432502	140.178619	4	2000	4
21	198	2	5	1.1076	48.170094	0	1700	4
22	170	4	5	0.5016	38.395699	0	2000	4
23	198	3	5	0.9801	47.392895	0	5810	6
24	184	3	5	0.59	42.775898	0	1700	4
25	282	3	5	3.320699	75.094879	0	1960	4
26	154	3	4	0.796	36.7309	0	2000	4
27	360	5	8	1.7613	89.796967	0	5000	5
28	164	2	3	1.49	44.776596	0	2850	5
29	192	1	3	1.9685	53.773788	0	4000	5
30	182	1	4	1.2219	46.598293	0	2000	4
31	152	1	3	1.2133	40.046295	0	1000	4
32	192	1	4	1.333	49.327793	0	3800	5
33	272	2	4	3.285398	78.245575	0	1560	4
34	278	2	4	3.539799	76.055077	0	2450	5
35	292	1	4	3.842798	80.942276	0	5000	5
36	414	1	1	8.024803	128.216736	1	890	4
37	576	4	6	5.849	160.850357	3	8000	6
38	442	1	2	8.364703	133.335754	2	2000	4
39	448	3	3	6.190401	131.090347	2	8	2
40	442	2	2	6.997202	132.061554	2	2000	4
41	456	2	3	7.089501	132.611557	2	2610	5
42	472	3	4	6.2044	134.071365	2	2000	4
43	456	2	3	7.233601	132.68158	2	2000	4
44	472	3	4	6.2044	134.071381	2	2000	4
45	454	1	3	7.297701	131.611771	2	2160	5
46	426	1	1	8.168903	130.719757	2	70000	6
47	664	0	2	14.201112	204.905441	3	339	4
48	472	3	4	6.206	134.093353	2	2000	4
49	648	3	7	8.184502	181.659683	3	3800	5
50	618	3	6	8.175901	175.107651	3	9960	6
51	646	3	6	9.171604	185.792709	3	3800	5
52	456	2	3	7.089501	132.611557	2	2000	4
53	488	4	5	5.1752	135.461182	2	2000	4
54	1408	16	32	-3.227797	325.685516	4	4000	5

ISSN 2616-0684 (Print)
ISSN 2616-0692 (Electronic)

55	1274	14	27	-1.027496	302.292877	4	4000	5
56	1246	13	27	-1.051995	293.052063	4	4000	5
57	1264	13	25	0.970802	308.960114	4	5000	5
58	780	6	11	5.4344	207.331268	5	4000	5
59	666	14	21	-9.7488	133.886139	4	51	3
60	844	17	27	-11.993001	167.604752	4	1000	4
61	1006	20	32	-14.168802	200.238358	4	1000	4
62	1168	23	37	-16.344606	232.871994	4	1000	4
63	410	0	0	10.605007	140.060028	2	5000	5
64	174	4	5	-1.5162	38.356194	0	9000	6
65	386	5	8	-0.576	95.565948	0	1750	4
66	254	0	0	7.267802	85.219963	1	750	3
67	352	0	0	9.998506	117.53894	1	750	3
68	282	0	0	8.048003	94.453957	1	750	3
69	244	4	4	0.5864	65.416176	0	2340	5
70	328	1	8	0.57274	71.43029	0	3800	5

Table 2 presents the calculated binding affinities and interaction modes of the docking complexes between the ligands and PDE4B protein. The binding affinities of all studied compounds with the target protein PDE4B exhibited high negative values, ranging from -10.88 to -5.651 kcal/mol. Among these, compound 49 had the strongest binding affinity (-10.88 kcal/mol), and 34 compounds outperformed the reference compound 1S1 (-7.49 kcal/mol). The top five compounds with binding affinities stronger than -9.5 kcal/mol were selected for molecular interaction analysis, as shown in Figure 1 and Table 2. Notably, compound 49 exhibited the strongest binding affinity with PDE4B (-10.88 kcal/mol), primarily due to hydrophobic interactions such as alkyl and pi-alkyl interactions with residues Ile410, Met347, Met431, Leu303, Ile450, and Phe446, as well as pi-pi stacked and pi-pi T-shaped interactions with Phe414 and Phe446. The interactions with Met431, Phe446, and Phe414 were also observed in the reference compound 1S1. Compound 2 also displayed a high binding affinity (-10.09 kcal/mol), forming crucial hydrogen bonds with Asp392, Thr345, Asn395, and Gln443, along with pi-pi stacked and pi-pi T-shaped interactions with Tyr233 and Phe446. The hydrogen bond with Asn395 and the pi-pi stacked and pi-pi T-shaped interactions with Tyr233 and Phe446 in compound 2 were similar to those of the reference compound, suggesting a potential inhibitory effect in the active site of PDE4B. Compounds 45 and 51 exhibited slightly lower binding affinities (-9.644 kcal/mol and -9.525 kcal/mol, respectively) but still demonstrated significant binding potential to PDE4B. Compound 45 formed a hydrogen bond with Asn395, supported by hydrophobic interactions (alkyl and pi-alkyl) with His234, Tyr233, Ile410, Phe414, and Met347, along with a pi-sigma interaction with Phe446. Meanwhile, compound 51 formed hydrogen bonds with Asp392 and His234, along with strong hydrophobic interactions with Phe414, Met347, Met431, Pro430, Ile450, and Phe446. Compared to the reference compound 1VV, both compounds 45 and 51 interacted with Asn395. Additionally, compound 51 showed an interaction with Asp392, similar to the reference 1VV-PDE4B complex. Furthermore, the interaction profiles of the selected *Ludwigia*-derived compounds were further compared with those of known PDE4B inhibitors. Roflumilast, an FDA-approved PDE4 inhibitor used in the treatment of chronic obstructive pulmonary disease (COPD), forms key contacts with residues such as Gln443, Asn395, Met411, Phe414, Met431, and Phe446 [31,32]. Similarly, Cilomilast used for respiratory disorders like asthma and COPD interacts with Gln443, Met411, Phe414, Met431, Met347, Leu393, and Phe446 [31,32]. Taken together, these findings suggest that the selected *Ludwigia*-derived compounds bind stably within the active site of PDE4B. Their strong binding affinities and diverse interaction profiles with critical amino acid residues highlight their promise as potential PDE4B inhibitors for further biological validation.

Molecular dynamics and binding free energies

After evaluating the molecular docking results of the studied compounds, MD simulations were further performed for the most potential complexes with the target protein PDE4B to assess their dynamic behavior and stability by analyzing RMSD parameters [33]. The results presented in Figure 2 show the changes in RMSD values of the protein backbone and ligands in the studied complexes. Specifically, the analysis of RMSD plots of the protein backbone in the complexes indicates that the values exhibit stability and are quite similar to the reference system and apo protein, with an average RMSD ranging from 0.152 to 0.301 nm throughout the 100 ns simulation. Meanwhile, the average RMSD values of the studied ligands 2, 16, 45, 49, and 51 in the complexes were 0.181 nm, 0.088 nm, 0.104 nm, 0.187 nm, and 0.173 nm, respectively, while the RMSD value of the reference compound 1S1 was 0.148 nm. It can be observed that the RMSD values of the studied ligands in the complexes are all below 0.2 nm (2 Å), indicating their stability at the active sites of the protein, demonstrating good binding stability. Overall, the RMSD analysis suggests that the studied compounds form stable complexes with PDE4B, maintaining their positions at the active site throughout the simulation. The analysis of root mean square fluctuation (RMSF) for individual amino acid residues provides critical insights into the structural dynamics and flexibility of protein-ligand complexes. RMSF quantifies the average deviation of each residue from its reference position during molecular dynamics simulations, where elevated values reflect increased local flexibility and potential structural perturbations upon ligand binding [33]. In this study, RMSF calculations were performed for the target protein in complex with a series of compounds, including ligands 2, 6, 16, 45, 49, and 51, as well as the apo form and the ref structure. The resulting data are visualized in Figure 3, highlighting variations across specific functional regions of the protein, namely the metal binding pocket (H234, H238, H274, D275, H278, N283, L303, E304, D346, M347, D392), the Q switch and P clamp pocket (Y233, L393, N395, W406, T407, I410, M411, M431, V439, S442, Q443, F446), and the solvent-filled side pocket (G280, S282, E413, F414, Q417, S429, C432) [34]. Among the investigated complexes, compounds 16 and 49 demonstrated the most significant impact on protein flexibility, particularly in residues M431, V439, S442, and C432, which showed markedly elevated RMSF values compared to both the apo and ref states. This suggests that these compounds induce localized conformational mobility within the Q switch/P clamp and solvent-filled side pockets, potentially altering the accessibility or configuration of the binding site. In contrast, ligands 2 and 6 showed RMSF profiles that closely resembled the ref structure, maintaining relatively low fluctuations across active site residues and thereby indicating a stabilizing interaction with the protein. Compounds 45 and 51 exhibited moderate increases in flexibility, particularly at loop-associated residues such as Q417 and S429, implying partial perturbation in local dynamics without extensive destabilization. The apo form, in the absence of any ligand, presented with moderate RMSF values across all active regions, whereas the ref configuration exhibited the lowest overall RMSF, reflecting a highly stable conformation.

ISSN 2616-0684 (Print)
ISSN 2616-0692 (Electronic)

Table 2: Binding affinity and interaction analysis of top hit compounds in the PDE4B active site pocket

ID	Compounds	Binding affinity (kcal/mol)	Interacting amino acid residues	Types of interactions
2	Quercetin-3-O-α-L-rhamnoside	-10.09	Asp392, Thr345, Asn395, Gln443	Hydrogen bond
			Ile410	Pi-alkyl
			Tyr233, Phe446	Pi-pi stacked and pi-pi T-shaped
			Asp392	Carbon hydrogen bond
16	Luteolin-8-C-glycoside	-9.585	Glu304, Gln443	Hydrogen bond
			Phe414, Phe446, Ile410	Alkyl and pi-alkyl
			His234	Pi-cation
45	Betulonic acid	-9.644	Asn395	Hydrogen bond
			His234, Tyr233, Ile410, Phe414, Met347	Alkyl and pi-alkyl
			Phe446	Pi-sigma
49	(23*E*)-feruloylhederagenin	-10.88	Ile410, Met347, Met431, Leu303, Ile450, Phe446	Alkyl and Pi-alkyl
			Phe414, Phe446	Pi-pi stacked and pi-pi T-shaped
			Asn395	Carbon hydrogen bond
51	(23Z)-feruloylhederagenin	-9.525	Asp392, His234	Hydrogen bond
			Phe414, Met347, Met431, Pro430, Ile450	Alkyl and Pi-alkyl
			Phe446	Pi-sigma
Ref.	2-ethyl-2-{[4-(methylamino)-6-(1H-1,2,4-triazol-1-yl)-1,3,5-triazin-2-yl]amino}butanenitrile	-7.49	Asn395, Gln443	Hydrogen bond
			Ile410, Met347, Tyr233, His234	Alkyl and Pi-alkyl
			Met431	Pi-sulfur
			Phe446, Phe414	Pi-pi stacked and pi-pi T-shaped
			Thr407, Gln443	Carbon hydrogen bond

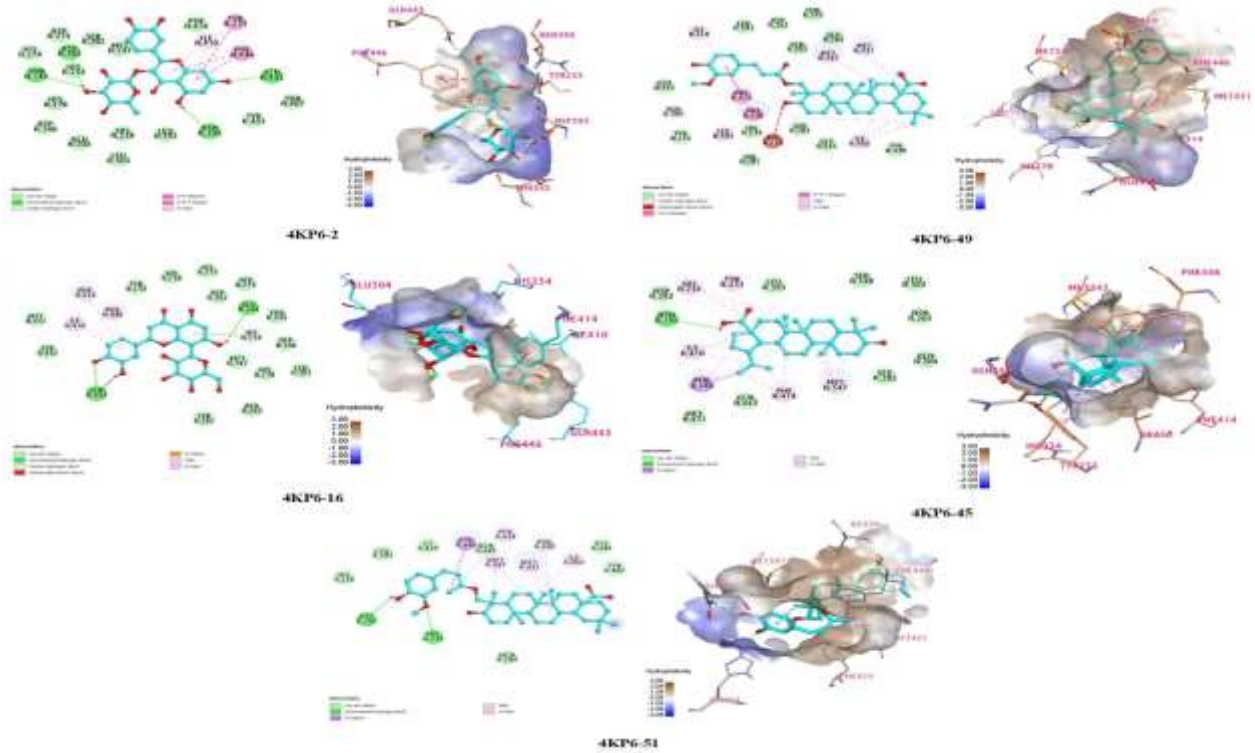

Figure 1: Binding mode of top hit compounds inside the active site pocket of PDE4B

ISSN 2616-0684 (Print)
ISSN 2616-0692 (Electronic)

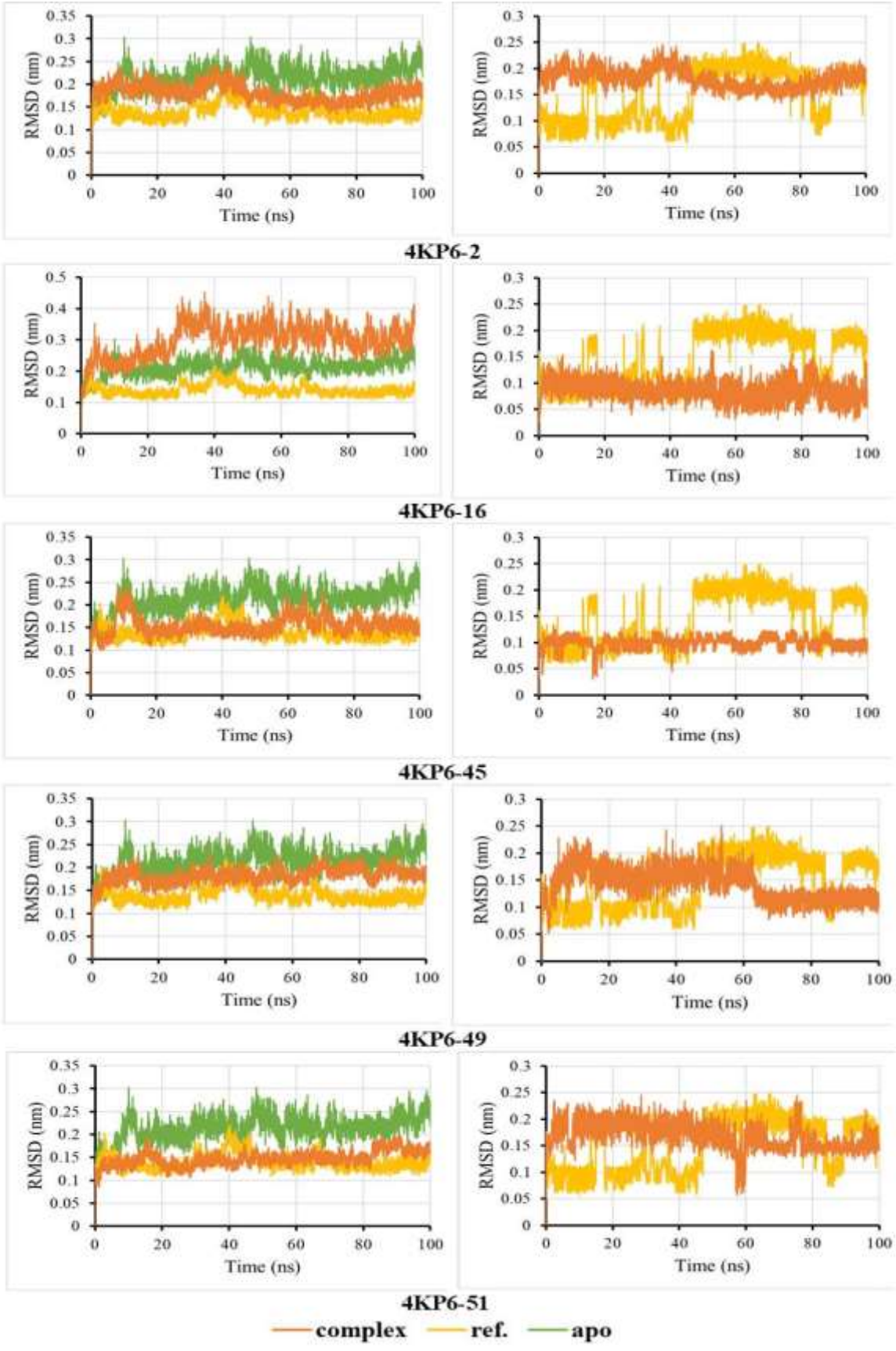

Figure 2: Root Mean Square Deviation (RMSD) plots of protein backbone (left) and ligand (right) in PDE4B complexes with top hit compounds

ISSN 2616-0684 (Print)
ISSN 2616-0692 (Electronic)

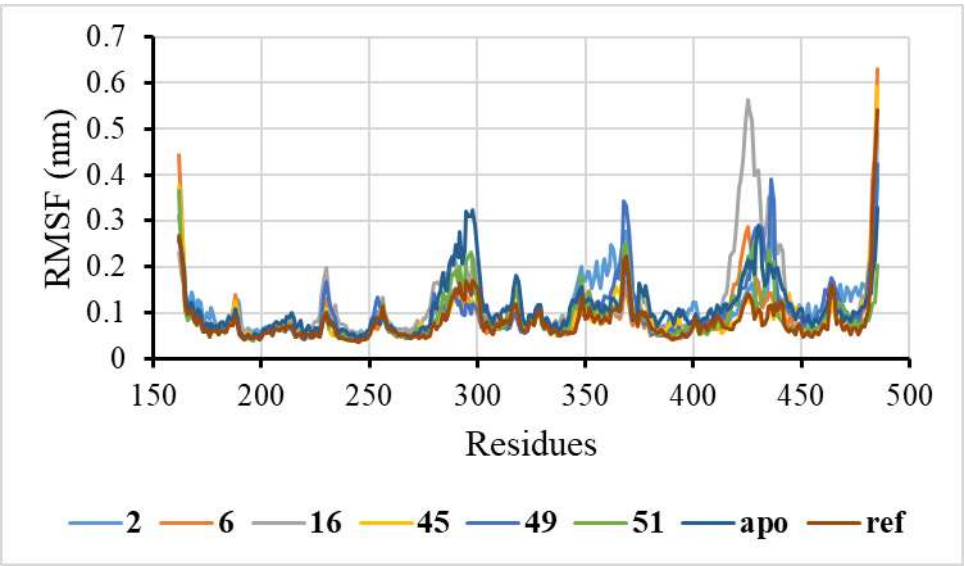

Figure 3: Root Mean Square Fluctuation (RMSF) plots of protein in PDE4B complexes with top hit compounds

This comparative pattern underscores the dynamic influence of ligand binding, with some compounds enhancing flexibility in key pockets, potentially facilitating functional rearrangements, while others promote structural stabilization. Notably, residues within the metal binding pocket remained relatively rigid across all systems, with only slight increases in RMSF observed under the influence of ligands 16 and 49, indicating that this region maintains its integrity despite ligand-induced perturbations elsewhere. Taken together, these results demonstrate that RMSF patterns vary significantly depending on the bound compound, with ligands 16 and 49 eliciting the greatest structural fluctuations, and ligands 2 and 6 exerting a stabilizing effect comparable to the reference model. This analysis provides valuable insights into how distinct ligands modulate the conformational dynamics of the protein, which may have functional implications for binding affinity, specificity, and catalytic efficiency. However, to further assess the strength and stability of their interactions, MMGBSA binding energy calculations were performed [35, 36]. The MMGBSA results revealed significant differences in binding affinity compared to the reference compound 1S1 (Figure 4). The total binding free energy (ΔG_{total}) of the compounds ranged from -54.2 to -24.7 kcal/mol. Among them, compound 49 had the lowest ΔG_{total} value of -54.2201 kcal/mol, indicating the strongest binding affinity with PDE4B. This could be attributed to the significant contribution of Van der Waals energy (-63.0033 kcal/mol) and gas-phase energy (-61.6217 kcal/mol), which help stabilize the complex. Compound 2 (ΔG_{total} = -45.9158 kcal/mol) and compound 16 (ΔG_{total} = -43.582 kcal/mol) also showed better binding affinity than the reference compound 1S1, with compound 2 having a significantly lower binding free energy due to the strong contribution of Van der Waals interactions and electrostatic energy. In contrast, compound 45 had a ΔG_{total} of -34.6974 kcal/mol, higher than the reference, indicating weaker binding capability. The main reason for this could be the excessively high electrostatic energy (EEL = 335.398 kcal/mol), which is counterbalanced by a very high polar solvation energy (EGB = -320.4618 kcal/mol), reducing the stability of the complex. Additionally, compound 51 had the highest ΔG_{total} of -24.7442 kcal/mol among all compounds, suggesting the weakest binding affinity. This may be due to the large negative solvation energy (-226.2 kcal/mol), significantly reducing the stability of the complex with PDE4B. Overall, the combination of RMSD and MMGBSA analyses indicates that compounds 2, 16, and 49 exhibit strong stability and favorable binding affinities with PDE4B, making those promising candidates for PDE4B inhibition. Among them, compound 49 demonstrates the strongest binding affinity and could serve as a potential lead compound for developing an effective PDE4B inhibitor.

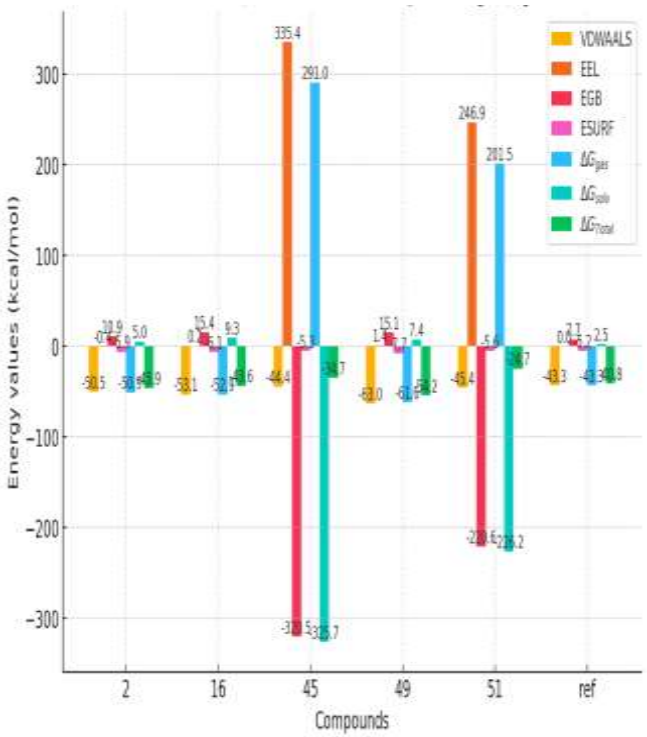

Figure 4: The binding free energy (kcal.mol^{-1}) for the studied systems, estimated via MM–GBSA calculations

Conclusion

This study provides valuable computational insights into the potential of *Ludwigia L.* phytochemicals as PDE4B inhibitors, offering a foundation for further drug development. By applying Lipinski's Rule, compounds with favorable drug-like properties and oral bioavailability were identified, while toxicity assessments ensured the selection of safer candidates. Molecular docking analysis highlighted several compounds with strong binding affinities for PDE4B, with compound 49 exhibiting the most promising inhibitory potential. Further validation through molecular dynamics simulations confirmed the stability of selected compounds within the PDE4B binding site, and MMGBSA binding energy calculations reinforced the high binding

affinity of compound 49. These findings suggest that *Ludwigia L.* derived compounds, particularly compound 49, could serve as promising lead molecules for PDE4B inhibition. However, experimental validation through *in vitro* and *in vivo* studies is necessary to confirm their biological activity, pharmacokinetics, and safety profiles. Future research should focus on optimizing the structural properties of these compounds to enhance their therapeutic potential and further explore their mechanisms of action in PDE4B inhibition. This study lays the groundwork for developing novel anti-inflammatory or respiratory disorder treatments based on *Ludwigia L.* phytochemicals.

Conflict of Interest

The authors declare no conflict of interest.

Authors' Declaration

The authors hereby declare that the work presented in this article is original and that any liability for claims relating to the content of this article will be borne by them.

Acknowledgements

The authors would like to acknowledge Thai Nguyen University, Vietnam for their support and assistance through the project with the code: ĐH2024-TN11-0: ĐH2024-TN11-01

Funding

The author(s) disclosed receipt of the following financial support for the research, authorship, and/or publication of this article: This study was financially supported under the project with the code: ĐH2024-TN11-01 by Thai Nguyen University, Vietnam.

References

1. POWO (2025). *Ludwigia* L. Plants of the World Online. Facilitated by the Royal BotanicGardens,Kew.Availablefrom: https://powo.science.kew.org/taxon/urn:lsid:ipni.org:names:30000573-2
2. Kirtikar KR, Basu BD. Indian Medicinal Plants. 2nd ed. India: International Book Distributors; 1999. p. 1088–1089.
3. Ghani A. Medicinal Plants of Bangladesh. 2nd ed. Dhaka: Asiatic Society of Bangladesh; 2003.
4. Perry LM. Medicinal Plants of East and South East Asia: Attributed Properties and Uses. Cambridge, MA: MIT Press; 1980. p. 294.
5. Khan MH, Yadava PS. Antidiabetic plants used in Thoubal district of Manipur, Northeast India. Indian J Tradit Knowl. 2010;9:510–514.
6. Ramírez G, Zavala M, Pérez J, Zamilpa A. In vitro screening of medicinal plants used in Mexico as antidiabetics with glucosidase and lipase inhibitory activities. Evid Based Complement Alternat Med. 2012;2012:701261.
7. Ipor I. *Ludwigia octovalvis* (Jacq.) P.H. Raven. In: van Valkenburg JLC, Bunyapraphatsara N, editors. Plant Resources of South-East Asia No. 12(2): Medicinal and Poisonous Plants 2. Leiden: Backhuys; 2001.
8. Murugesan T, Sinha S, Pal M, Saha B. Review on phytochemical and medicinal aspects of *Jussiaea suberuticosa* Linn. Anc Sci Life. 2002;21:205–207.
9. Shaphiullah M, Bachar SC, Kundu JK, Begum F, Uddin MA, Roy SC, Khan M. Antidiarrheal activity of the methanol extract of *Ludwigia hyssopifolia* Linn. Pak J Pharm Sci. 2003;16(1):7–11.
10. Houslay MD. PDE4 cAMP-specific phosphodiesterases. Cell Signal. 2001;13(9):655–663.
11. Fertig BA, Baillie GS. PDE4-mediated cAMP signalling. J Cardiovasc Dev Dis. 2018;5(1):8.
12. Zervoudakis G, Chou J, Gurney ME, Quesnelle KM. PDE4 subtypes in cancer. Oncogene. 2020;39(19):3791–3802.
13. Menniti FS, Faraci WS, Schmidt CJ. Phosphodiesterases in the CNS: targets for drug development. Nat Rev Drug Discov. 2006;5(8):660–670.
14. Donders Z, Skorupska IJ, Willems E, Mussen F, Van Broeckhoven J, Carlier A. Beyond PDE4 inhibition: A comprehensive review on downstream cAMP signaling in the central nervous system. Biomed Pharmacother. 2024;177:117009.
15. Su Y, Ding J, Yang F, He C, Xu Y, Zhu X. The regulatory role of PDE4B in the progression of inflammatory function study. Front Pharmacol. 2022;13:982130.
16. Blauvelt A, Langley RG, Gordon KB, Silverberg JI, Eyerich K, Sommer MO. Next generation PDE4 inhibitors that selectively target PDE4B/D subtypes: A narrative review. Dermatol Ther. 2023;13(12):3031–3042.
17. Dastidar SG, Rajagopal D, Ray A. Therapeutic benefit of PDE4 inhibitors in inflammatory diseases. Curr Opin Investig Drugs. 2007;8(5):364–372.
18. Fan T, Wang W, Wang Y, Zeng M, Liu Y, Zhu S, Yang L. PDE4 inhibitors: potential protective effects in inflammation and vascular diseases. Front Pharmacol. 2024;15:1407871.
19. Lipinski CA. Lead- and drug-like compounds: the rule-of-five revolution. Drug Discov Today Technol. 2004;1(4):337–341.
20. Jayaram B, Singh T, Mukherjee G, Mathur A, Shekhar S, Shekhar V. Sanjeevini: a freely accessible web-server for target directed lead molecule discovery. BMC Bioinformatics. 2012;13(Suppl 7):S7.
21. Banerjee P, Kemmler E, Dunkel M, Preissner R. ProTox 3.0: a webserver for the prediction of toxicity of chemicals. Nucleic Acids Res. 2024;52(W1):W513–W520.
22. Halgren TA. MMFF VI. MMFF94s option for energy minimization studies. J Comput Chem. 1999;20(7):720–729.
23. O'Boyle NM, Banck M, James CA, Morley C, Vandermeersch T, Hutchison GR. Open Babel: an open chemical toolbox. J Cheminform. 2011;3:33.
24. Gewald R, Grunwald C, Egerland U. Discovery of triazines as potent, selective and orally active PDE4 inhibitors. Bioorg Med Chem Lett. 2013;23(15):4308–4314.
25. Trott O, Olson AJ. AutoDock Vina: improving the speed and accuracy of docking with a new scoring function, efficient optimization, and multithreading. J Comput Chem. 2010;31(2):455–461.
26. Eberhardt J, Santos-Martins D, Tillack AF, Forli S. AutoDock Vina 1.2.0: New docking methods, expanded force field, and python bindings. J Chem Inf Model. 2021;61(8):3891–3898.
27. Abraham MJ, Murtola T, Schulz R, Páll S, Smith JC, Hess B, Lindahl E. GROMACS: High performance molecular simulations through multi-level parallelism from laptops to supercomputers. SoftwareX. 2015;1:19–25.
28. Valdés-Tresanco MS, Valdés-Tresanco ME, Valiente PA, Moreno E. gmx_MMPBSA: a new tool to perform end-state free energy calculations with GROMACS. J Chem Theory Comput. 2021;17(10):6281–6291.
29. Lipinski CA. Lead- and drug-like compounds: the rule-of-five revolution. Drug Discov Today Technol. 2004;1(4):337–341. (Duplicate of ref. 19; nên bỏ 1).
30. Hoang Minh Chau C, Thi Tra Giang N, Thi Thuy Tram N, Thi My Chau L, Xuan Ha N, Thi Thuy P. In silico molecular docking and molecular dynamics of *Prinsepia utilis* phytochemicals as potential inhibitors of phosphodiesterase 4B. J Chem Res. 2024;48(6):17475198241305879.
31. Gavaldà A, Roberts RS. Phosphodiesterase-4 inhibitors: a review of current developments (2010–2012). Expert Opin Ther Pat. 2013;23(8):997–1016.
32. Kwak HJ, Nam KH. Molecular properties of phosphodiesterase 4 and its inhibition by roflumilast and cilomilast. Molecules. 2025;30(3):692.
33. Filipe HA, Loura LM. Molecular dynamics simulations: advances and applications. Molecules. 2022;27(7):2105.

ISSN 2616-0684 (Print)
ISSN 2616-0692 (Electronic)

34. Card GL, England BP, Suzuki Y, Fong D, Powell B, Lee B. Structural basis for the activity of drugs that inhibit phosphodiesterases. Structure. 2004;12(12):2233–2247.
35. Wang E, Sun H, Wang J, Wang Z, Liu H, Zhang JZ, Hou T. End-point binding free energy calculation with MM/PBSA and MM/GBSA: strategies and applications in drug design. Chem Rev. 2019;119(16):9478–9508.
36. Genheden S, Ryde U. The MM/PBSA and MM/GBSA methods to estimate ligand-binding affinities. Expert Opin Drug Discov. 2015;10(5):449–461.
37. Shawky EM, Elgindi M, Hassan MM. Phytochemical and biological diversity of genus *Ludwigia*: A comprehensive review. ERU Res J. 2023;2(3):447–474.
38. Shilpi JA, Gray AI, Seidel V. Chemical constituents from *Ludwigia adscendens*. Biochem Syst Ecol. 2010;38(1):106–109.
39. Chang CI, Kuo CC, Chang JY, Kuo YH. Three new oleanane-type triterpenes from *Ludwigia octovalvis* with cytotoxic activity against two human cancer cell lines. J Nat Prod. 2004;67(1):91–93.